INTERNATIONAL JOURNAL FOR NUMERICAL METHODS IN ENGINEERING
Int. J. Numer. Meth. Engng 2003; **56**:1931–1948 (DOI: 10.1002/nme.642)

Boundary knot method for 2D and 3D Helmholtz and convection–diffusion problems under complicated geometry

Y. C. Hon[1] and W. Chen[2,3,*,†]

[1]*Department of Mathematics, City University of Hong Kong, Hong Kong SAR, China*
[2]*Simula Research Laboratory, P.O. Box 134, Lysaker NO-1325, Norway*
[3]*Institute of Mechanics, Chinese Academy of Sciences, 15 Bei-Si-Huan Xi Rd, Beijing 100080, China*

SUMMARY

The boundary knot method (BKM) of very recent origin is an inherently meshless, integration-free, boundary-type, radial basis function collocation technique for the numerical discretization of general partial differential equation systems. Unlike the method of fundamental solutions, the use of non-singular general solution in the BKM avoids the unnecessary requirement of constructing a controversial artificial boundary outside the physical domain. The purpose of this paper is to extend the BKM to solve 2D Helmholtz and convection–diffusion problems under rather complicated irregular geometry. The method is also first applied to 3D problems. Numerical experiments validate that the BKM can produce highly accurate solutions using a relatively small number of knots. For inhomogeneous cases, some inner knots are found necessary to guarantee accuracy and stability. The stability and convergence of the BKM are numerically illustrated and the completeness issue is also discussed. Copyright © 2003 John Wiley & Sons, Ltd.

KEY WORDS: boundary knot method; radial basis function; non-singular general solution; method of fundamental solutions; dual reciprocity method; boundary element; meshless

1. INTRODUCTION

The meshless numerical techniques have in recent years become increasingly popular since the construction of a mesh in the standard finite element and boundary element methods is not a trivial work especially for non-linear, moving boundary and higher-dimensional problems [1–3]. Among these meshless techniques, the local boundary integral equation (MLBIE) method [4], the boundary node method (BNM) [5], and the method of fundamental solutions (MFS) [3, 6] are typically meshless boundary-type numerical schemes. The essence of the meshless MLBIE and BNM is basically a combination of the moving least square (MLS) technique with variant boundary element schemes, whereas the MFS is a boundary-type radial

*Correspondence to: W. Chen, Simula Research Laboratory, P.O. Box 134, Lysaker NO-1325, Norway.
†E-mail: wenc@simula.no

Contract/grant sponsor: Strategic Research, City University of Hong Kong; Contract/grant number: 7001051

Received 15 August 2001
Revised 2 November 2001
Accepted 14 June 2002

basis function (RBF) collocation scheme. Both the MLBIE and the BNM involve singular integration and hence are mathematically more complicated in comparing with the commonly used finite element method (FEM). In addition, their low order approximations also lower computational efficiency [3]. In fact, since the BNM still requires meshes in its numerical integration, it is not a truly meshless scheme like those MLS-based meshless FEMs [4, 7]. The MLBIE does not require a mesh at all but is not easily used. On the other hand, the MFS possesses integration-free, spectral convergence, easy-to-use, inherently meshfree merits [3, 6]. However, the requirement of an arbitrary fictitious boundary outside the physical domain to avoid the singularity of the fundamental solution hinders its practical applicability [3, 8]. In particular, applying the MFS to complex-shaped boundary problems requires the tricky location of source knots in terms of boundary conditions and geometry [9] and often leads to severe ill-conditioning of the resulting interpolation matrix [10].

Chen and Tanaka [11, 12] recently developed a boundary knot method (BKM) as an alternative boundary-type meshless RBF collocation scheme. The BKM is basically a combination of the Trefftz-type technique [13] with the RBF, non-singular general solution, and dual reciprocity method (DRM). The RBF is employed in the BKM to approximate the inhomogeneous terms via the DRM, while the non-singular general solution of the partial differential operator leads to a boundary-only RBF formulation for the homogeneous solution. It is worth stressing that the BKM eliminates the inherent fatal inefficiency of the MFS. Namely, the use of the non-singular general solution in the BKM instead of singular fundamental solution in the MFS avoids the construction of a controversial artificial boundary. It is noted [12] that as compared with the dual reciprocity boundary element method (DR-BEM) [14, 15] and the MFS [3], the BKM is theoretically flexible to general linear and non-linear inhomogeneous partial differential equations. Moreover, due to the use of the radial basis function, the BKM is essentially meshless for solving any dimensional problems [11]. In addition, the method is mathematically simple and easy to implement.

Owing to its very recent origin, the method has so far merely been applied to linear and non-linear Dirichlet problems defined on a smooth 2D elliptic domain [11, 12, 16]. This paper aims to extend the BKM to 2D Helmholtz and convection–diffusion problems under rather complicated domains with irregular boundaries. This will also be a first time the BKM is shown to be effective in solving 3D problems. Since applying the DRM and RBF to approximation of particular solution is now a rather mature technique, this paper only gives an inhomogeneous example to illustrate that the inner knots are absolutely necessary to ensure the solution stability and accuracy. This observation is at odd with a controversial argument given in Reference [15] and other literature that the inner knots are not always necessary in the DRM except for improving accuracy. It is noted that the emphasis of this study is concerned with various 2D complex-shaped boundary geometry and 3D problems. Numerical experiments presented are very encouraging in terms of efficiency, accuracy, stability, and simplicity. The stability and convergence rate of the method are also numerically illustrated. Some open issues on completeness, condition number, and convergence are raised in Section 4.

2. BOUNDARY KNOT METHOD

The BKM can be illustrated by a two-step numerical approach [11, 12]. Firstly, the DRM and RBF are employed to evaluate the particular solution of the problem, and secondly, its

homogeneous solution is calculated by using non-singular general solution formulation. Without loss of generality, consider the following multi-dimensional convection–diffusion equation

$$D\nabla^2 u(x) + \mathbf{v} \bullet \nabla u(x) - k u(x) = f(x) \tag{1}$$

$$u(x) = R(x), \quad x \in S_u \tag{2a}$$

$$\frac{\partial u(x)}{\partial n} = N(x), \quad x \in S_T \tag{2b}$$

where $\mathbf{v}$ denotes a velocity vector, D is the diffusivity coefficient, k represents the reaction coefficient, S_u and S_T denote the boundaries with the Dirichlet and Neumann conditions, respectively, x is the multi-dimensional independent variable and n the unit outward normal. The solution $u(x)$ can be expressed as

$$u(x) = u_{\mathrm{h}}(x) + u_{\mathrm{p}}(x) \tag{3}$$

where $u_{\mathrm{h}}(x)$ and $u_{\mathrm{p}}(x)$ are the homogeneous and particular solutions of the problem, respectively. In other words, the particular solution $u_{\mathrm{p}}(x)$ satisfies

$$D(x)\nabla^2 u_{\mathrm{p}}(x) + \mathbf{v} \bullet \nabla u_{\mathrm{p}}(x) - k u_{\mathrm{p}}(x) = f(x) \tag{4}$$

but does not necessarily satisfy the boundary conditions. The homogeneous solution $u_{\mathrm{h}}(x)$ satisfies

$$D\nabla^2 u_{\mathrm{h}}(x) + \mathbf{v} \bullet \nabla u_{\mathrm{h}}(x) - k u_{\mathrm{h}}(x) = 0 \tag{5}$$

$$u_{\mathrm{h}}(x) = R(x) - u_{\mathrm{p}}(x), \quad x \in S_u \tag{6a}$$

$$\frac{\partial u_{\mathrm{h}}(x)}{\partial n} = N(x) - \frac{\partial u_{\mathrm{p}}(x)}{\partial n}, \quad x \in S_T \tag{6b}$$

The computation for these particular and homogeneous solutions by using a two-step BKM scheme will be introduced in the following sections.

2.1. Particular solution by the DRM and RBF

Based on the DRM and RBF [14, 15], the inhomogeneous term $f(x)$ of Equation (4) can be approximated by

$$f(x) \cong \sum_{k=1}^{N+L} \alpha_k \phi(r_k) \tag{7}$$

where α_k are the unknown coefficients to be determined, N and L represent, respectively, the total numbers of knots on the domain and the boundary, $r_k = \|x - x_k\|$ denotes the Euclidean distance between each x and x_k, and ϕ denotes a RBF, which we will specify in the later example part. It is noted that different from the RBF-based Kansa method, the augmented polynomial terms are missing in Equation (7). This is because that Li [17] proved very recently that the invertibilility of the dual reciprocity interpolation matrix does not require

such augmented polynomial terms with conditionally positive definite MQ RBF. Our numerical examples also show that the augmented polynomial terms are not necessary with the DRM and various RBFs we have used. The difference between the DRM and the Kansa's method lies in that the former does not involve any boundary conditions. On the other hand, the interpolation conditions of the RBF approach has been discussed in many publications. For instance, see Reference [18].

From Equation (7) we can uniquely determine each α_k by

$$\alpha = A_\phi^{-1}\{f(x_i)\} \tag{8}$$

where A_ϕ is a $(N+L)\times(N+L)$ non-singular RBF interpolation matrix. From Equation (8), the particular solution $u_\mathrm{p}(x)$ at any points can be obtained by summing all the localized particular solutions

$$u_\mathrm{p}(x) = \sum_{k=1}^{N+L} \alpha_k \psi(r_k) \tag{9}$$

where each $\psi(r_k)$ satisfies the equation

$$\phi(r) = D\nabla^2\psi(r) + \mathbf{v}\bullet\nabla\psi(r) - k\psi(r) \tag{10}$$

In general, it is not a trivial task to integrate Equation (10) to obtain the approximated particular solution ψ for an arbitrary RBF ϕ [3]. Recently, Muleskov *et al.* [19] derived an analytic formula to compute the approximated particular solutions for Helmholtz operator by using the polyharmonic splines as the RBF ϕ. Unfortunately, in the case of convection–diffusion operator, such analytical approximation is still not available now. In our practical computation, we apply a reverse procedure for the particular solution $\psi(r_k)$ of Equation (1). Namely, the approximated particular solution ψ is specified beforehand, and then the corresponding RBF ϕ is evaluated by simply substituting the specified ψ into Equation (10). This scheme also works well for various types of problems with the dual reciprocity BEM [20, 21].

2.2. *Boundary formulation with non-singular general solution*

The homogeneous solution u_h from Equations (5) and (6a), (6b) can be obtained by using various boundary-type numerical techniques [3, 15]. In the BKM, we employ a non-singular general solution instead of a singular fundamental solution in the standard BEM. For illustration, in the case of the convection–diffusion operator, the non-singular general solution is as follow:

$$u_n^{\#}(r) = \frac{1}{2\pi}\left(\frac{\mu}{2\pi r}\right)^{(n/2)-1} \mathrm{e}^{-\mathbf{v}\cdot\mathbf{r}/2D} I_{(n/2)-1}(\mu r), \quad n \geqslant 2 \tag{11}$$

For comparison, the corresponding fundamental solution is given by

$$u_n^{*}(r) = \frac{1}{2\pi}\left(\frac{\mu}{2\pi r}\right)^{(n/2)-1} \mathrm{e}^{-\mathbf{v}\cdot\mathbf{r}/2D} K_{(n/2)-1}(\mu r), \quad n \geqslant 2 \tag{12}$$

where n is the dimension of the problem; I and K, are respectively, the modified Bessel functions of the first kind and the second kind; and

$$\mu = \left[\left(\frac{|\mathbf{v}|}{2D}\right)^2 + \frac{k}{D}\right]^{1/2} \tag{13}$$

It is not difficult via any symbolic software package such as Maple to verify that the general solution (11) satisfies the following homogeneous convection–diffusion equation

$$D\nabla^2 u_n^{\#} + \mathbf{v} \bullet \nabla u_n^{\#} - k u_n^{\#} = 0 \tag{14}$$

The only difference between the non-singular general solution and the singular fundamental solution is that the former uses the modified Bessel function of the first kind whereas the latter uses instead the modified Bessel function of the second kind. It is noted that the fundamental solution (12) has a singularity at the origin.

Let $\{x_j\}_{j=1}^{L}$ represent a set of knots on the physical boundary. The homogeneous solution $u_{\mathrm{h}}(x)$ of Equation (5) can be approximated by the following series:

$$u_{\mathrm{h}} = \sum_{j=1}^{L} \beta_j u_n^{\#}(r_j) \tag{15}$$

where $r_j = \|x - x_j\|$, L is the total number of boundary knots, β_j are unknown coefficients to be determined. Collocating Equations (6a) and (6b) in terms of the series (15) produces

$$\sum_{j=1}^{L} \beta_j u_n^{\#}(r_{ij}) = R(x_i) - u_{\mathrm{p}}(x_i) \tag{16a}$$

$$\sum_{j=1}^{L} \beta_j \frac{\partial u_n^{\#}(r_{mj})}{\partial n} = N(x_m) - \frac{\partial u_{\mathrm{p}}(x_m)}{\partial n} \tag{16b}$$

where i and m indicate the Dirichlet and Neumann boundary response knots respectively. In the case where the inner knots are used, we need to constitute a set of supplementary equations for the unknowns as follow:

$$\sum_{j=1}^{L} \beta_j u_n^{\#}(r_{lj}) = u(x_l) - u_{\mathrm{p}}(x_l), \quad l = 1, \ldots, N \tag{17}$$

where l denotes the index of each internal response knot and N is the total number of interior points. We have then obtained a total of $N + L$ simultaneous algebraic equations. By solving the simultaneous equations (16a), (16b) and (17), we obtain the values of the undetermined coefficients β_j and the solutions values at the N internal knots. Once this is done, it is straightforward to calculate u value at any inner knot by

$$u(x) = u_{\mathrm{h}}(x) + u_{\mathrm{p}}(x) = \sum_{j=1}^{L} \beta_j u_n^{\#}(r_j) + \sum_{k=1}^{N+L} \alpha_k \psi(r_k) \tag{18}$$

Unlike the MFS, all boundary collocation knots x_j in the BKM are placed only on the physical boundary and can be treated as either source or response points. It is straightforward to extend the above solution procedure to the other differential operators such as the Helmholtz, modified Helmholtz, and biharmonic operators [11, 15].

As was pointed out in References [3, 22], the DRM with the RBF is a meshless technique for evaluating particular solution of general PDEs. The non-singular general solution formulation in the BKM for homogeneous solution is also an essentially meshless RBF boundary-type

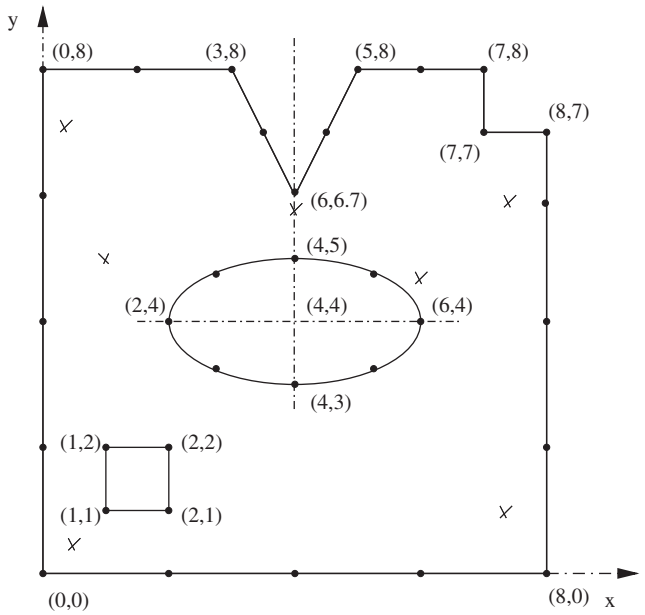

Figure 1. Configuration of 2D irregular geometry.

methodology. Thus, the proposed two-step BKM scheme constructs a truly meshless numerical discretization technique for general higher-dimensional problems.

3. APPLICATIONS AND DISCUSSIONS

In this section the applications of the BKM to solve both 2D and 3D Helmholtz and conv ection–diffusion problems will be illustrated. As was mentioned earlier, the main purpose of this paper is to verify the applicability of the BKM to solve PDE problems with arbitrarily irregular boundary. In the BKM, the inhomogeneous term is approximated by using the DRM and RBF which is similar to DRBEM and MFS. Therefore, the major emphasis on the BKM solution is on its applicability to finding the solutions of the corresponding homogeneous problems. In this paper, an inhomogeneous case is given to indicate that some internal knots are necessary for the DRM evaluation of the particular solution in the BKM solution of inhomogeneous problems. The application of the BKM to more complicated inhomogeneous problems is very straightforward [12, 16]. Furthermore, to the knowledge of the authors, this paper gives the first attempt to apply the BKM to solve 3D problems.

Unless otherwise specified, all 2D tested cases have the same configuration of irregular geometry shown in Figure 1with Neumann conditions at $x = 0$ and $y = 0$ boundary and Dirichlet conditions at otherwise boundary portions. It is also noted that this configuration involves corners, sharp notches, and interior elliptical and rectangular cut-outs. These interior and exterior boundary shapes are deliberately designed to verify the robustness of the BKM in solving arbitrary complicated geometric problems. For the 3D case, the configuration is given in

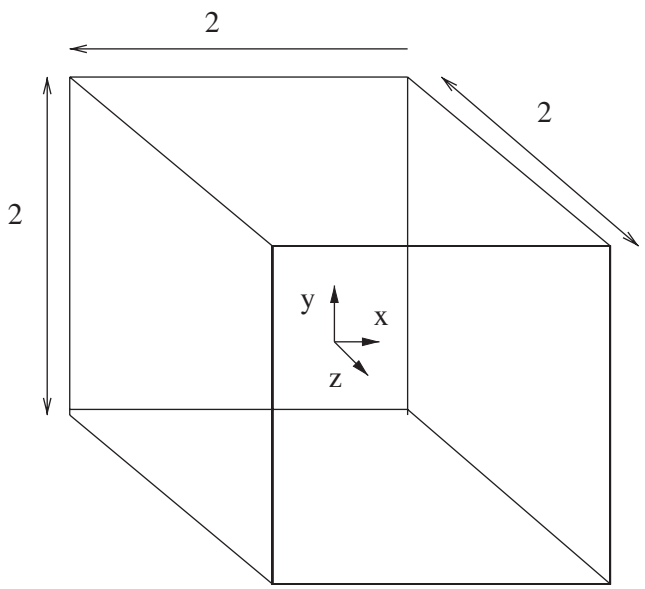

Figure 2. Configuration of a cube.

Figure 2 which is a 3D cube with all sides of equal length. Both the Helmholtz and convection–diffusion problems with this 3D cube geometry are tested to verify the simplicity, efficiency, and accuracy of the BKM for solving higher-dimensional problems. The present experimental problems were taken from Reference [15] with some modifications.

All tested results are displayed in Tables I–V. The relative error of the BKM solution, which is defined to be the ratio of the approximation error to the value of the analytical solution, are shown under the columns of BKM $(L+N)$, where L and N are, respectively, the total numbers of boundary and inner knots. The quantities under the column *Exact* are the exact solutions. In Figure 1, the small blank circles denote the boundary discretization knots, while the tiny crosses represent the inner knots.

3.1. A 2D homogeneous Helmholtz problem

We first consider a homogeneous Helmholtz problem

$$\frac{\partial^2 u}{\partial x^2}+\frac{\partial^2 u}{\partial y^2}+\lambda^2 u=0, \quad x, y \in \Omega \tag{19}$$

subject to the following boundary conditions

$$u(x, y)=R(x, y), \quad x, y \in S_u \tag{20}$$

$$\frac{\partial u(x, y)}{\partial n}=N(x, y), \quad x, y \in S_T \tag{21}$$

Three cases with analytical solutions

$$u(x, y) = \sin(x)\sin(y) \tag{22a}$$

$$u(x, y) = x\sin(\sqrt{2}y) \tag{22b}$$

$$u(x, y) = \sin(10x) + \sin(10y) \tag{22c}$$

are tested. The above Dirichlet and Neumann boundary conditions $R(x, y)$ and $N(x, y)$ can be evaluated easily by using the corresponding analytical solutions (22a), (22b) and (22c). The non-singular solution of the 2D homogeneous Helmholtz operator is

$$\sigma(r) = J_0(\eta r) \tag{23}$$

where J_0 is the zero order Bessel function of the first kind and η is the wave number. For the above three cases, η is taken to be $\sqrt{2}$, $\sqrt{2}$, and 10, respectively.

From the numerical relative errors of the BKM solutions with incremental boundary knots given in Tables I(a)–(c), we find that the BKM is a stable, accurate and rapidly convergent numerical technique. It is noted that only boundary knots were required in the homogeneous cases. It is also observed that the BKM results with only 29 knots were very accurate for the cases (22a) and (22b) with small wave number, while the cases (22c) with higher wave number need relatively more knots to attain the same accurate BKM results. Taking the consideration of the complicated exterior and interior contours, the accuracy of the proposed BKM solution is very satisfactory.

3.2. An inhomogeneous Helmholtz problem

To investigate the effect of the inner knots to the solution of the inhomogeneous problems, we consider the following problem

$$\frac{\partial^2 u}{\partial x^2} + \frac{\partial^2 u}{\partial y^2} + u = x, \quad (x, y) \in \Omega \tag{24}$$

$$u(x, y) = R(x, y), \quad (x, y) \in S_u \tag{25}$$

$$\frac{\partial u(x, y)}{\partial n} = N(x, y), \quad (x, y) \in S_T \tag{26}$$

The analytical solution is

$$u(x, y) = \sin x + \sin y + x \tag{27}$$

Similar to the previous case, the boundary conditions $R(x, y)$ and $N(x, y)$ can be determined from the exact solution (27). Here the rather simple inhomogeneous term is deliberately chosen to show that even for such a smooth linear inhomogeneous term, some inner knots are also required in finding the BKM solution. The DRM and RBF were employed to evaluate the particular solution. In terms of the mulitquadratic (MQ) RBF, the chosen approximated particular solution for Equation (9) is

$$\psi(r) = (r^2 + c^2)^{3/2} \tag{28}$$

Table I.

(a) Relative errors for 2D homogeneous Helmholtz problem with analytical solution (22a).

X	Y	Exact	BKM (25)	BKM (29)	BKM (33)
0.5	0.5	0.230	−7.0e − 3	−2.5e − 4	−1.1e − 6
4.0	6.0	0.211	5.4e − 4	4.8e − 5	−2.5e − 7
6.0	4.5	0.273	4.0e − 3	−2.5e − 4	2.0e − 6
1.0	4.0	−0.637	−4.1e − 5	1.9e − 5	−2.1e − 7
7.5	6.0	−0.262	1.2e − 2	−1.2e − 3	2.1e − 5
0.5	7.0	0.315	5.7e − 4	1.1e − 3	2.1e − 5
7.5	1.0	0.789	−2.5e − 2	3.3e − 3	2.1e − 5

(b) Relative errors for 2D homogeneous Helmholtz problem with analytical solution (22b).

X	Y	Exact	BKM (25)	BKM (29)	BKM (41)
0.5	0.5	0.325	7.4e − 2	−2.4e − 3	−6.6e − 6
4.0	6.0	3.229	−5.9e − 4	1.8e − 5	−3.7e − 7
6.0	4.5	0.484	−4.4e − 2	−1.1e − 3	1.7e − 6
1.0	4.0	−0.586	1.6e − 2	1.3e − 3	4.7e − 7
7.5	6.0	6.054	1.2e − 2	4.2e − 4	3.2e − 7
0.5	7.0	−0.229	2.4e − 2	−1.1e − 2	2.1e − 5
7.5	1.0	7.408	4.5e − 2	2.5e − 3	−8.0e − 7

(c) Relative errors for 2D homogeneous Helmholtz problem with analytical solution (22c).

X	Y	Exact	BKM (121)	BKM (129)	BKM (149)
0.5	0.5	−1.918	−3.9e − 4	7.3e − 6	9.7e − 9
4.0	6.0	0.440	−5.3e − 4	8.2e − 6	6.3e − 7
6.0	4.5	0.546	−4.2e − 4	2.4e − 6	3.7e − 8
1.0	4.0	0.201	2.5e − 3	−1.2e − 6	1.1e − 6
7.5	6.0	−0.693	4.8e − 5	−3.2e − 6	4.8e − 9
0.5	7.0	−0.185	1.9e − 3	1.2e − 4	5.0e − 6
7.5	1.0	−0.932	2.9e − 4	−6.0e − 6	9.8e − 8

where c is called the shape parameter. In applying Equation (10), the corresponding MQ-like radial basis function is

$$\phi(r) = 6(r^2 + c^2) + \frac{3r^2}{\sqrt{r^2 + c^2}} + (r^2 + c^2)^{3/2} \tag{29}$$

The particular solution is then evaluated by using formulas (8) and (9). Compared with other radial basis functions such as the thin plate spline, the MQ enjoys a spectral convergence [23]. However, the accuracy of the solution greatly depends on the optimal value of the shape parameter c, which is often problem-dependent [24]. An analytical formula for the value of the optimal c remains an open issue. See Chen and Tanaka [11, 16] for some latest developments on how to construct an efficient RBF.

Table II(a) lists the BKM results without using inner knots. The nearly optimal shape parameters c is obtained by trial-and-error to be 3, 2, 1 for the cases with 21, 25, and 27 knots, respectively. It can be observed from the tables that as the knot density increases, the

Table II.

(a) Relative errors for 2D inhomogeneous Helmholtz problem without inner knot.

X	Y	Exact	BKM (21)	BKM (25)	BKM (29)
0.5	0.5	1.459	−7.6e − 2	6.4e − 3	6.0e − 3
4.0	6.0	2.964	−2.9e − 3	9.7e − 5	2.1e − 4
6.0	4.5	4.743	−7.6e − 4	−2.5e − 3	−2.5e − 3
1.0	4.0	1.085	−2.5e − 2	−9.0e − 3	−9.8e − 3
7.5	6.0	8.159	−1.3e − 2	−1.1e − 2	−3.7e − 3
0.5	7.0	1.636	−2.0e − 1	−3.4e − 2	−5.6e − 2
7.5	1.0	9.279	5.7e − 2	−2.1e − 3	2.7e − 2

(b) Relative errors for 2D inhomogeneous Helmholtz problem with 7 inner knots.

X	Y	Exact	BKM (17+7)	BKM (21+7)	BKM (25+7)
0.5	0.5	1.459	6.4e − 3	3.7e − 5	−1.5e − 6
4.0	6.0	2.964	−5.1e − 4	2.9e − 6	−3.2e − 6
6.0	4.5	4.743	7.2e − 4	8.1e − 6	−1.6e − 6
1.0	4.0	1.085	3.3e − 3	5.4e − 4	1.2e − 4
7.5	6.0	8.159	−6.7e − 4	−9.9e − 6	−1.9e − 5
0.5	7.0	1.636	1.0e − 2	−1.2e − 3	−5.2e − 4
7.5	1.0	9.279	−1.4e − 2	1.0e − 4	−3.5e − 6

(c) Relative errors for 2D inhomogeneous Helmholtz problem with 1 inner knot.

X	Y	Exact	BKM (17+1)	BKM (21+1)	BKM (25+1)
0.5	0.5	1.459	5.8e − 3	−4.6e − 4	−3.4e − 5
4.0	6.0	2.964	−5.2e − 4	−5.7e − 6	−1.1e − 6
6.0	4.5	4.743	7.2e − 4	2.5e − 5	2.2e − 6
1.0	4.0	1.085	3.1e − 3	1.4e − 3	5.0e − 5
7.5	6.0	8.159	−6.4e − 4	9.8e − 5	−2.1e − 5
0.5	7.0	1.636	1.1e − 2	−3.1e − 3	−1.2e − 4
7.5	1.0	9.279	−1.5e − 2	1.2e − 4	−1.0e − 4

optimal value of the shape parameter decreases. It is also observed that these BKM solutions converge unstably and slowly. Unlike the previous homogeneous case, the BKM results were not much improved even with more knots. Table II(b) instead gives the solutions by using an additional 7 interior knots. The locations of these interior knots are listed in the first and second columns of Table II(b). The BKM solutions at these knots are used to compare their relative errors against the exact ones. In sharp contrast to those without inner knots as given in Table II(a), it can be observed that the BKM solution by using the additional 7 inner knots has a much faster and stable convergence rate for the present inhomogeneous problem. In addition, the MQ shape parameter c is all set to 9 in these computations but the BKM solution accuracy seems not sensitive to the parameter c if inner knots are used. Furthermore, the BKM results with only one interior knot are given in Table II(c). Similar to the case of using 7 inner knots, the shape parameter of the MQ is all taken as 15 irrespective of the total number of knots. Comparing the results given in Tables II(a)–(c), we can conclude that the

more inner knots are used, the more accurate and stable the BKM solutions are. Moreover, with the use of inner knots, the MQ shape parameter in the BKM solution is not sensitive to the knot density.

In this inhomogeneous case, it is particularly worth noting that the BKM with one inner knot performed much better than without any inner knots. This indicates that inner knots are indispensable to guarantee the stability and accuracy in the DRM and RBF evaluation of the particular solutions in the proposed two-steps BKM scheme. Since the DRBEM also applies the DRM to calculate the particular solution, the argument given in Reference [15] that except for improving the solution accuracy the interior knots are not necessary in the DRBEM is in doubt.

3.3. A 2D homogeneous convection–diffusion problem

The numerical solution of convection–diffusion problem is often a difficult task due to the troublesome convection terms. It has been claimed that the BEM performs better than the FEM and FDM in solving the convection–diffusion problems due to the fact that the convection terms have been inherently included into the fundamental solution for the convection–diffusion operator. This is also expected to be true to the proposed BKM scheme. For illustration, we consider the applicability of the BKM scheme in using the non-singular general solution of the convection–diffusion operator to the following homogeneous problem

$$\nabla^2 u = -\partial u/\partial x - \partial u/\partial y \tag{30}$$

with boundary conditions

$$u(x, y) = R(x, y), \quad x, y \in S_u \tag{31}$$

$$\frac{\partial u(x, y)}{\partial n} = N(x, y), \quad x, y \in S_T \tag{32}$$

The analytical solution is given to be

$$u(x, y) = \mathrm{e}^{-x} + \mathrm{e}^{-y} \tag{33}$$

Again the boundary values can be determined from the analytical solution (33). The BKM [11] using the non-singular general solution of Helmholtz operator was also successfully employed to solve the above problem in a smooth elliptical domain and under a Dirichlet boundary condition, where the DRM was used to evaluate the particular solution due to the convection terms. In this study we used the non-singular general solution of the convection–diffusion operator as shown in Equation (11). In addition, the present experiments can handle much more complex-shaped boundary with both Neumann and Dirichlet conditions.

The relative errors of the BKM solutions are summarized in Table III. It is noted that the BKM results using 17 boundary knots achieved in average an accuracy up to the fourth significant digits. In contrast, the DRBEM with 16 boundary knots and 17 interior points [15] produced a less accurate solution for the same homogeneous convection–diffusion problem under a much simpler smooth elliptical domain and Dirichlet boundary conditions. The use of the Laplacian fundamental solution and the lower order of convergence ratio of the BEM are blamed for this inefficiency of the DRBEM. It should be pointed out that the present BKM solutions are also better than the BKM solutions with the non-singular solution of

Table III. Relative errors for 2D homogeneous convection–diffusion problem.

X	Y	Exact	BKM (17)	BKM (21)	BKM (25)
0.5	0.5	1.213	−1.3e − 3	3.3e − 7	6.5e − 7
4.0	6.0	0.021	3.2e − 6	−4.2e − 9	1.3e − 8
6.0	4.5	0.014	5.9e − 5	−3.5e − 8	−6.9e − 8
1.0	4.0	0.386	−3.1e − 5	3.7e − 7	−8.8e − 8
7.5	6.0	0.003	−4.2e − 4	3.8e − 6	−1.2e − 6
0.5	7.0	0.607	2.0e − 5	−1.3e − 6	2.2e − 7
7.5	1.0	0.368	−1.7e − 3	−1.5e − 6	1.1e − 6

Helmholtz operator. This striking accuracy here is because the present proposed BKM with the convection–diffusion non-singular solution could well capture the convective effects of the convection–diffusion system.

3.4. A 3D homogeneous Helmholtz problem

Three-dimensional problems are usually not easy to deal with partly due to the expensive effort in the mesh generation for mesh-dependent techniques and, more importantly, due to the exponential increasing size of resulting analogous equations. This fact is the so-called curse of dimensionality. The objective of the following experiment is to verify numerically the accuracy and efficiency of the BKM in handling 3D case. Consider

$$\frac{\partial^2 u}{\partial x^2} + \frac{\partial^2 u}{\partial y^2} + \frac{\partial^2 u}{\partial z^2} + \lambda^2 u = 0, \quad (x, y, z) \in \Omega \tag{34}$$

with the Dirichlet boundary conditions

$$u(x, y, z) = R(x, y, z), (x, y, z) \in S_u \tag{35}$$

The two cases with analytical solution are given, respectively, by

$$u(x, y, z) = \sin(x)\cos(y)\cos(z) \tag{36a}$$

for an unit sphere domain, and

$$u(x, y, z) = \sin(x) + \sin(y) + \sin(z) \tag{36b}$$

for a cube domain. The non-singular solutions of 3D homogeneous Helmholtz operator are

$$\sigma(r) = \frac{\sin(\eta r)}{r} \tag{37}$$

where η are chosen to be $\sqrt{3}$. The relative errors of the BKM solutions are tabulated in Tables IV(a) and (b). It can be observed from the tables that the BKM worked equally well for this 3D problem as in the previous 2D cases. Based on some numerical experiments and theoretical analysis concerning the dimensional effect on the error bounds of the RBF interpolation, Chen and He [25] conjectured that the RBF-based numerical scheme may circumvent the curse of dimensionality like the Monte Carlo method. To be more precise, the computational effort in using the RBF on solving higher-dimensional problems only grows

Table IV.

(a) Relative errors for 3D homogeneous Helmholtz problem with sphere domain.

X	Y	Z	Exact	BKM (15)	BKM (50)
0.0	0.0	0.0	0.0	−2.4e − 3	−3.6e − 5
0.2	0.0	0.0	0.199	1.8e − 2	2.2e − 4
−0.4	0.0	0.0	−0.389	−2.7e − 3	−2.9e − 5
0.5	0.0	0.0	0.479	1.3e − 2	6.4e − 5
−0.6	0.0	0.0	−0.565	−8.9e − 4	1.2e − 5
0.8	0.0	0.0	0.717	1.5e − 2	−1.6e − 4
−0.9	0.0	0.0	−0.783	7.9e − 5	2.3e − 5

(b) Relative errors for 3D homogeneous Helmholtz problem with cubic domain.

X	Y	Z	Exact	BKM (14)	BKM (22)
−0.4	−0.5	−0.5	−1.348	3.6e − 4	7.6e − 4
−0.5	−0.5	0.8	−0.241	8.3e − 3	9.4e − 3
−0.6	0.99	0.5	−0.751	−1.3e − 3	8.9e − 4
0.7	0.5	0.5	1.603	4.9e − 4	7.0e − 4
0.0	0.75	0.2	0.483	−1.1e − 3	−8.2e − 4
0.0	−0.25	0.8	0.470	−1.4e − 3	−2.0e − 3
0.0	0.0	0.0	0.0	8.2e − 14	−7.1e − 15

linearly instead of exponentially. Kansa and Hon [26] in their numerical tests also observed that the RBF collocation method seems to enjoy this computational advantage. For numerical verifications, it can be seen from Tables IV(a) and (b) that the BKM with only tens points produced rather accurate solutions for the 3D problems. This indicates that the BKM may be a new alternative to tackle high-dimensional problems with relatively much smaller number of knots.

3.5. A 3D homogeneous convection–diffusion problem

We expand the previous 2D convection–diffusion problem to a 3D case:

$$\frac{\partial^2 u}{\partial x^2} + \frac{\partial^2 u}{\partial y^2} + \frac{\partial^2 u}{\partial z^2} = -\frac{\partial u}{\partial x} - \frac{\partial u}{\partial y} - \frac{\partial u}{\partial z} \tag{38}$$

subject to the Dirichlet boundary condition

$$u(x, y, z) = R(x, y, z), \quad (x, y, z) \in S_u \tag{39}$$

The analytical solution is

$$u(x, y, z) = \mathrm{e}^{-x} + \mathrm{e}^{-y} + \mathrm{e}^{-z} \tag{40}$$

and the corresponding non-singular general solution is given by

$$\sigma_n(r) = \mathrm{e}^{-\frac{\mathbf{v}\cdot\mathbf{r}}{2D}} \frac{\sinh(r\sqrt{3}/2)}{r} \tag{41}$$

Table V. Results for 3D homogeneous convection–diffusion problem.

X	Y	Z	Exact	BKM (14)	BKM (22)
−0.4	−0.5	−0.5	4.789	3.0e − 3	1.0E − 3
−0.5	−0.5	0.8	3.747	−2.0e − 3	−1.1E − 3
−0.6	0.99	0.5	2.800	−4.0e − 4	2.8E − 4
0.7	0.5	0.5	1.710	1.4e − 3	3.6E − 4
0.0	0.75	0.2	2.694	−5.8e − 4	1.6E − 5
0.0	−0.25	0.8	2.733	−7.4e − 4	−6.7E − 5
0.0	0.0	0.0	3.000	−6.0e − 5	−6.0E − 5

where **r** is the distance vector between the source and response knots and **v** is the velocity vector $\{1, 1, 1\}^{\mathrm{T}}$.

Table V lists the BKM solution errors against the analytical solutions. The BKM average relative errors at some specified 7 inner knots with a total of 14 and 22 boundary knots are, respectively, 1.2e − 3 and 4.1e − 4. These accurate results numerically illustrate the superior convergence speed and accuracy of the BKM. For comparison, the DRBEM was also applied to solve the same problem with the use of the Laplace fundamental solution and the DRM for the evaluation of the particular solution of convection terms [15]. Although a total of 74 boundary and 27 interior knots were used in these DRBEM methods, the accuracy of the solution was inferior to that of the BKM with only 14 knots, the reason is that the Laplacian does not take the convective terms into the boundary formulation and the BEM suffers from its lower order accuracy. An interesting fact observed from Table V is that the more apart of the inner knots from the boundary, the more accurate is the BKM solution.

4. COMPLETENESS, CONVERGENCE, AND CONDITIONING NUMBER

4.1. Completeness issue

The n-dimensional homogeneous Helmholtz equation is given by

$$\nabla^2 u + \lambda^2 u = \begin{cases} -\Delta_i, & \text{in } \Omega \\ 0, & \end{cases} \tag{42}$$

where Δ_i represents the Dirac delta function at a source point i corresponding to its fundamental solution versus zero for its general solution.

$$u^*(r) = \frac{1}{4}\left(\frac{\lambda}{2\pi r}\right)^{n/2-1} [Y_{n/2-1}(\lambda r) - \mathrm{i}\, J_{n/2-1}(\lambda r)] \tag{43}$$

is its complete fundamental solution [27–29], where J and Y are, respectively, the Bessel function of the first and second kinds. The Bessel function J is C^∞ smooth while the Bessel function Y encounters a singularity at the origin. The non-singular general solution can be interpreted as the non-singular imaginary part of the above complete complex singular fundamental solution. In practical computing of the BEM, the singular real part of (43) is usually used as the fundamental solution. This raised the completeness issue of both the BEM and

BKM solutions. Chen and Tanaka [12, 16] discussed this issue by comparing the BKM to the multiple reciprocity BEM (MRM) with the Laplace fundamental solution plus its high-order terms, where, in contrast, only the singular real part of the complex fundamental solution (43) is applied [28]. DeMey [30] also successfully employed the BEM with the singular real part to calculate the Helmholtz eigenvalue problems that circumvented any complex calculation and had the advantage to circumvent any complex calculation. However, as was pointed out in References [31, 32], the BEM with only the real part of the Helmholtz complex fundamental solution may converge to spurious eigenvalues in some cases. Chen *et al*. [32] also provided some remedies to cure this inefficiency. Kamiya and Andoh [28] pointed out that the MRM with the Laplacian fundamental solution does not satisfy the Sommerfeld radiation conditions at infinity. Power [29] discussed the incompleteness issue of the MRM in performing the Brinkman equation.

The incompleteness concerns on the MRM and BEM with the real part of the Helmholtz fundamental solution may also apply to the BKM solution of the Helmholtz problem. However, we note that the eigensolutions of a practical Helmholtz problem can usually be expressed only by smooth Bessel function of the first kind rather than singular Bessel function of the second kind. For example, the exact Helmholtz eigenfunctions on the unit disk are series of the Bessel functions of the first kind [33, pp. 378–379]. In other words, only the non-singular general solution is used to avoid the singularity at the origin in many practical computations involving symmetrical circular and cylindrical domain problems. This provides some intuitive explanations on the feasibility of the BKM. The BKM is therefore expected to be applicable to a broader range of Helmholtz problems than the MRM and BEM. Although a thorough theoretical analysis on this issue is not an easy task, more numerical experiments will be beneficial to the early development stage of the BKM method.

On the other hand, in the case of the modified Helmholtz problems, we note that there is no such completeness issue as in the Helmholtz problem. The non-singular general solution [16] and singular fundamental solution [27] are, respectively,

$$u_n^{\#}(r) = \frac{1}{2\pi}\left(\frac{\lambda}{2\pi r}\right)^{(n/2)-1} I_{(n/2)-1}(\lambda r), \quad n \geqslant 2 \tag{44}$$

and

$$u_n^{*}(r) = \frac{1}{2\pi}\left(\frac{\lambda}{2\pi r}\right)^{(n/2)-1} K_{(n/2)-1}(\lambda r), \quad n \geqslant 2 \tag{45}$$

We could not even be sure of the completeness of the solutions (44) or (45). The same difficulty occurs in the convection–diffusion case as shown in the previous formulas (11) and (12). An immediate question in both cases is whether or not the singularity is essential to attain the reliable solutions by the boundary-type discretization schemes.

4.2. Convergence and conditioning number

Like all global numerical schemes, the large dense interpolation matrix resulted from using the RBF-based scheme usually suffers from severe ill-conditioning inefficiency [3, 26]. To further investigate this issue, Table VI displays the average relative errors and conditioning numbers of the BKM solutions of the previous 2D homogeneous Helmholtz and convection–diffusion

Table VI. Average relative errors and conditioning numbers for 2D homogeneous Helmholtz with analytical solution (22a) and convection–diffusion problems.

L	Err_H	Cond_H	Err_C	Cond_C
17	7.4e − 1	5.6e + 02	5.1e − 4	4.7e + 15
21	3.9e − 2	1.6e + 03	1.1e − 6	2.0e + 19
25	7.1e − 3	8.8e + 04	4.7e − 7	1.1e + 20
29	9.1e − 4	2.2e + 04	4.1e − 7	9.2e + 20
33	9.5e − 5	7.4e + 03	6.8e − 8	3.2e + 21
37	6.0e − 7	1.5e + 04	2.9e − 8	1.2e + 22
41	3.1e − 6	2.4e + 04	4.7e − 8	1.2e + 22

problems, with the columns under Err and Cond with lower case $_H$ and $_C$, respectively; and L is the total number of boundary knots. The average relative error is defined to be

$$\mathrm{err} = \frac{1}{N} \sum_{i=1}^{N} \left| \frac{u_i - \bar{u}_i}{u_i} \right| \tag{46}$$

where N is the total number of inner knots, u_i and $\bar{u}_i$ are, respectively, the exact and BKM solutions at these knots. The locations of these inner knots are the same as those indicated in Tables I–III. All computations were done on a Dell-PC Pentium III computer using the Microsoft Fortran Power Station 4.0 with double precision. The LU decomposition algorithm was employed to solve the resulting discretised system of equations.

It can be observed from Table VI that the convergence of the BKM solution was fast and stable. For a detailed numerical study of the BKM convergence behaviours see Reference [34]. It is also interesting to note that although the conditioning numbers of the convection–diffusion problem were much larger than those of the Helmholtz problem, the former in general has higher accuracy than the latter. In the case of the MFS, Golberg and Chen [3] has a similar observation. They pointed out that the irrelevances between the ill-conditioning of interpolation matrix and the high accuracy of the solution may be due to some inherent cancellation of round-off errors. By far an explicit theoretical explanation for this is still not available. Very interestingly, Fornberg and Wright [35] uses the complex shape parameter to significantly improve the stability and accuracy of the ill-conditioning MQ interpolation matrix. This may help ease the BKM ill-conditioning woe in the evaluation of the particular solution with the MQ-type RBFs. In addition, we found that in both examples, the conditioning numbers did not change rapidly with the increase of the boundary knots. In particular, unlike other global schemes, the conditioning number of the Helmholtz problem unexpectedly remained stably mild scale despite the increase of the knots. It is stressed here that we did not apply any special treatment to solve the resulting BKM discretization equations.

5. CONCLUSIONS

This work validated that the BKM consistently produces very accurate solutions for the 2D Helmholtz and convection–diffusion problems with rather complex-shaped interior and

exterior contours, which shows that unlike the MFS [10], the BKM is insensitive to geometric irregularity. The efficacy of the BKM to solve the 3D Helmholtz and convection–diffusion problems is also demonstrated. The BKM solutions are found to uniformly converge to the exact solutions in all testing cases. The illustrative experiments also manifested that for inhomogeneous problems, some inner knots were required to guarantee the stable convergence and high accuracy in the DRM and RBF evaluation of the particular solution.

The BKM is a new RBF-based boundary-type descritization technique with the remarkable merits of efficiency, high accuracy and stability, fast convergence, and mathematical simplicity. Similar to the domain-type RBF-based methods [23, 26], the essential meshless merit does give the BKM an edge over the BEM to easily handle higher-dimensional complicated-geometry problems by using only scattered knots. Moreover, the numerical experiments showed that the BKM could avoid the curse of dimensionality in the solution of the 3D problem. This attractive advantage is endorsed by the theoretical analysis and experimental findings that the use of higher order smooth radial basis functions can offset the dimensional affect [16, 25, 26].

The advantage of the BKM over the MFS is that the former eliminates the controversial requirement on the artificial boundary. The arbitrariness in the choice of the ambiguous fictitious boundary in the MFS may lead to some troublesome issues in the engineering computations. The BKM is therefore comparatively much more promising in the real world computing. Very recently, by analogy with the symmetric RBF Hermite interpolation scheme proposed in Reference [36], one of the present authors [37] developed the symmetric BKM scheme which has the symmetric interpolation matrix irrespective of boundary shape and conditions. Nonetheless, the BKM is still at its early development stage. Some concerns on the completeness, singularity and conditioning of the BKM interpolations are discussed with some open issues raised in this paper. Much more work will be needed to explore the full potential and possible limit of the method. The applications of the BKM to solve time-dependent and non-linear problems are presently under investigation.

ACKNOWLEDGEMENTS

The second author is grateful of a visiting research fellowship to Mathematical Department of City University of Hong Kong. This work was also partially supported by a strategic research grant number 7001051 of the City University of Hong Kong.

REFERENCES

1. Belytschko T, Lu YY, Gu L. Element-free Galerkin methods. *International Journal for Numerical Methods in Engineering* 1994; **37**:229–256.
2. Liu WK, Jun S, Zhang YF. Reproducing kernel particle methods. *International Journal for Numerical Methods in Engineering* 1995; **20**:1081–1106.
3. Golberg MA, Chen CS. The method of fundamental solutions for potential, Helmholtz and diffusion problems. In *Boundary Integral Methods—Numerical and Mathematical Aspects*, Golberg MA (ed.). Computational Mechanics Publications: Southampton, U.K., 1998; 103–176.
4. Atluri SN, Zhu T. New concepts in meshless methods. *International Journal for Numerical Methods in Engineering* 2000; **47**:537–556.
5. Mukherjee YX, Mukherjee S. The boundary node method for potential problems. *International Journal for Numerical Methods in Engineering* 1997; **40**:797–815.
6. Bogomolny A. Fundamental solutions method for elliptic boundary value problems. *SIAM Journal on Numerical Analysis* 1985; **22**(4):644–669.
7. Mendonca P, Barcellos C, Duarte A. Investigations on the hp-Cloud method by solving Timoshenko beam problems. *Computational Mechanics* 2000; **25**:286–295.

8. Kane JH. *Boundary Element Analysis in Engineering Continuum Mechanics*. Prentice-Hall: New Jersey, 1994.
9. Balakrishnan K, Ramachandran PA. A particular solution Trefftz method for non-linear Poisson problems in heat and mass transfer. *Journal of Computational Physics* 1999; **150**:239–267.
10. Kitagawa T. Asymptotic stability of the fundamental solution method. *Journal of Computational and Applied Mathematics* 1991; **38**:263–269.
11. Chen W, Tanaka M. New insights in boundary-only and domain-type RBF methods. *International Journal of Nonlinear Sciences and Numerical Simulation* 2000; **1**(3):145–152.
12. Chen W, Tanaka M. A meshless, integration-free, and boundary-only RBF technique. *Computers and Mathematics with Applications* 2002; **43**:379–391.
13. Piltner R. Recent development in the Trefftz method for finite element and boundary element application. *Advances in Engineering Software* 1995; **2**:107–115.
14. Nardini D, Brebbia CA. A new approach to free vibration analysis using boundary elements. *Applied Mathematical Modelling* 1983; **7**:157–162.
15. Partridge PW, Brebbia CA, Wrobel LW. *The Dual Reciprocity Boundary Element Method*. Computational Mechanics Publications: Southampton, U.K., 1992.
16. Chen W, Tanaka M. Relationship between boundary integral equation and radial basis function. In *The 52nd Symposium of JSCME on BEM*, Tanaka M (ed.). Tokyo, 2000.
17. Li J. Mathematical justification for RBF-MFS. *Engineering Analysis with Boundary Elements* 2001; **25**(10): 897–901.
18. Carr JC, Fright WR, Beatson RK. Surface interpolation with radial basis functions for medical imaging. *IEEE Transactions on Medical Imaging* 1997; **16**:96–107.
19. Muleskov AS, Golberg MA, Chen CS. Particular solutions of Helmholtz-type operators using higher order polyharmonic splines. *Computational Mechanics* 1999; **23**:411–419.
20. Wrobel LC, DeFigueiredo DB. A dual reciprocity boundary element formulation for convection–diffusion problems with variable velocity fields. *Engineering Analysis with Boundary Elements* 1991; **8**(6):312–319.
21. Kogl M, Gaul L. Dual reciprocity boundary element method for three-dimensional problems of dynamic piezoelectricity. In *Boundary Elements XXI*. CMP: Southampton, 1999; 537–548.
22. Partridge PW, Sensale B. The method of fundamental solutions with dual reciprocity for diffusion and diffusion-convection using subdomains. *Engineering Analysis with Boundary Elements* 2000; **24**:633–641.
23. Kansa EJ. Multiquadrics: a scattered data approximation scheme with applications to computational fluid-dynamics. *Computers and Mathematics with Applications* 1990; **19**:147–161.
24. Zerroukat M, Power H, Chen CS. A numerical method for heat transfer problems using collocation and radial basis function. *International Journal for Numerical Methods in Engineering* 1998; **42**:1263–1278.
25. Chen W, He J. A study on radial basis function and quasi-Monte Carlo methods. *International Journal of Nonlinear Sciences and Numerical Simulation* 2000; **1**(4):337–342.
26. Kansa EJ, Hon YC. Circumventing the ill-conditioning problem with multiquadric radial basis functions: applications to elliptic partial differential equations. *Computers and Mathematics with Applications* 2000; **39**: 123–137.
27. Kythe PK. *Fundamental Solutions for Differential Operators and Applications*. Birkhauser: Boston, 1996.
28. Kamiya N, Andoh E. A note on multiple reciprocity integral formulation for the Helmholtz equation. *Communications in Numerical Methods in Engineering* 1993; **9**:9–13.
29. Power H. On the completeness of the multiple reciprocity series approximation. *Communications in Numerical Methods in Engineering* 1995; **11**:665–674.
30. DeMay G. A simplified integral equation method for the calculation of eigenvalues of the Helmholtz equation. *International Journal for Numerical Methods in Engineering* 1977; **11**:1340–1342.
31. Nowak AJ, Neves AC (eds). *The Multiple Reciprocity Boundary Element Method*. Computational Mechanics Publication: Southampton, UK, 1994.
32. Chen JT, Huang CX, Chen KH. Determination of spurious eigenvalues and multiplicities of true eigenvalues using the real-part dual BEM. *Computational Mechanics* 1999; **24**:41–51.
33. Chen G, Zhou J. *Boundary Element Methods*. Academic Press: London, 1992.
34. Chen W, Hon YC. Numerical convergence of boundary knot method in the analysis of Helmholtz, modified Helmholtz, and convection–diffusion problems. *Computer Methods in Applied Mechanics and Engineering* 2002, accepted.
35. Fornberg B, Wright G. Stable computation of multiquadric interpolants for all values of the shape parameter. *BIT*, submitted.
36. Fasshauer GE. Solving partial differential equations by collocation with radial basis functions. In *Proceedings of Surface Fitting and Multiresolution Methods*, Mehaute A, Rabut C, Schumaker LL (eds). Vanderbilt University Press, 1997; 131–138.
37. Chen W, Symmetric boundary knot method. *Engineering Analysis with Boundary Elements* 2002; **26**(6): 489–494.

